

The Role of Elemental Sulfur and Chloride Ions on Pit Initiation at MnS Inclusion in Stainless Steel

Aya Chiba, Izumi Muto, Yu Sugawara, Nobuyoshi Hara

Department of Materials Science, Tohoku University
6-6-02, Aramaki, Aoba-ku, Sendai 980-8579, Japan

Sulfide inclusions such as MnS act as initiation sites of pitting on stainless steels in chloride-containing solutions. In our previous studies,¹⁻³ the trenches at the MnS/steel boundaries were found to be formed under anodic polarization and to act as a precursor of pits. It was also demonstrated that the dissolution of the steel side causes the trenches, and the pits initiate in the trenches. The trench formation is considered to be caused by the synergistic effect of the MnS dissolution products and Cl⁻ ions. Identifying the chemical composition of the MnS dissolution products and clarifying their electrochemical characteristic are of key importance to elucidate the pit initiation mechanism at the MnS inclusions in the stainless steels.

To analyze the dissolution products of the MnS inclusion, the microscopic anodic polarization was performed in 3 M NaCl, and then the microscopic Raman spectroscopy analysis was carried out in the solution at open circuit potential. Figure 1a shows the micro-scale electrode area examined. Type 303 stainless steel surface was masked using a resin. The electrode area contained a large MnS inclusion at the center. Figure 1b displays the microscopic anodic polarization curve in 3 M NaCl. The Raman spectrum at Point 1 in Fig. 1c (MnS/steel boundary) and the reference spectrum of sulfur powder are exhibited in Fig. 1d. The spectrum at Point 1 is similar to that of sulfur powder, which has sharp peaks at 150, 217, and 471 cm⁻¹. This result suggests that elemental sulfur is a dissolution product of the MnS inclusion. The Raman spectrum at Point 1 after rinsing with deionized water (Fig. 1e) and the reference spectrum of iron sulfide powder are shown in Fig. 1f. The spectrum at Point 1 (after rinsing) is similar to that of iron sulfide powder, which has a strong peak at 280 cm⁻¹. This result indicates that iron sulfide was generated on the steel surface at the boundary after the polarization.

To clarify the electrochemical reaction between stainless steel and elemental sulfur in the solution containing Cl⁻ ions, low-sulfur type 304 stainless steel was polarized in NaCl solution with elemental sulfur. Sulfur suspension was prepared by acidifying thiosulfate-containing solution to pH 3.5. In the solution containing elemental sulfur and Cl⁻ ions (3 M NaCl-1 mM Na₂S₂O₃ at pH 3.5), the anodic current rapidly increased with increasing potential from corrosion potential, indicating the active dissolution of the stainless steel was caused by the coexistence of elemental sulfur and Cl⁻ ions. In contrast, in the filtered solution of 3 M NaCl-1mM Na₂S₂O₃ at pH 3.5, in which elemental sulfur was removed, the stainless steel underwent passivation. In 3 M NaCl of pH 3.5 and 1 mM Na₂S₂O₃ of pH 3.5 (sulfur suspension), the stainless steel also passivated. It is clear that the synergistic effect of elemental sulfur and Cl⁻ ions caused the active dissolution of the stainless steel.

Based on these results, a pit initiation mechanism at the MnS inclusions has been proposed. On the stainless steel surfaces with the MnS inclusions, elemental sulfur produced by the dissolution of the MnS inclusions and Cl⁻ ions causes the dissolution of the steel matrix sides of the MnS/steel boundaries. The trenches produced by the dissolution of the steel matrix are extended to the depth direction with increasing potential in potentiodynamic polarization measurements. The hydrolysis reaction of Cr³⁺ released from the steel matrix proceeds, and the pH in the trenches decreases gradually. At the same time, the electrode potential at the bottom of the trenches decreases due to *IR-drop*. And then, the transition from passive to active occurs locally in the trenches. The local active dissolution generated in the trenches is thought to be pitting at MnS inclusions in chloride-containing solutions.

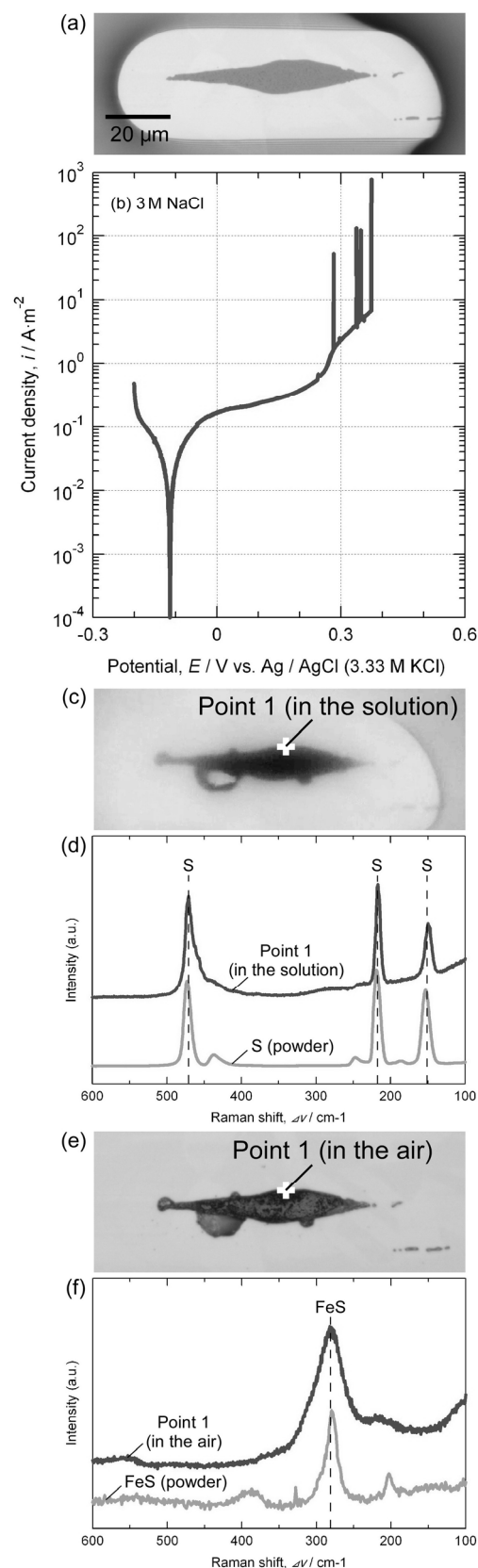


Figure 1. (a) Optical microscopy image of the micro-scale electrode area in the air before the polarization. (b) Polarization curve measured in 3 M NaCl at 298 K. (c) Optical microscopy image of the electrode area in the solution after the polarization. (d) Microscopic Raman spectrum at Point 1 in the solution and the reference spectrum of elemental sulfur. (e) Optical microscopy image of the electrode area in the air after rinsing with water. (f) Microscopic Raman spectrum at Point 1 in the air after rinsing with water and the reference spectrum of iron sulfide.

1. A. Chiba, I. Muto, Y. Sugawara, and N. Hara, *ECS Transactions – Boston, MA*, **41** (2012).
2. A. Chiba, I. Muto, Y. Sugawara, and N. Hara, *J. Electrochem. Soc.*, **159**, C341 (2012).
3. A. Chiba, I. Muto, Y. Sugawara, and N. Hara, *ECS Transactions – Honolulu, HI*, (2012).